Investigating the impact of motion in the scanner on brain age predictions

Roqaie Moqadam[1,2], Mahsa Dadar[*,1,2], Yashar Zeighami[*,1,2]

1. Department of Psychiatry, McGill University, Montreal, Quebec, Canada
2. Douglas Mental Health University Institute, Montreal, Quebec, Canada

***** These authors contributed equally to this work.

Corresponding Authors:

Yashar Zeighami, Douglas Mental Health University Institute, Montreal, Quebec, Canada
Roqaie Moqadam, Douglas Mental Health University Institute, Montreal, Quebec, Canada
emails: yashar.zegihami@mcgill.ca, roqaie.moqadam@umontreal.ca

Abstract

Introduction: Brain Age Gap (BAG) is defined as the difference between the brain's predicted age and the chronological age of an individual. Magnetic resonance imaging (MRI)-based BAG can quantify acceleration of brain aging, and is used to measure brain health as aging and disease interact. Motion in the scanner is a common occurrence that can affect the acquired MRI data and act as a major confound in the derived models. As such, age-related changes in head motion may impact the observed age-related differences. However, the relationship between head motion and BAG has not been directly examined. The aim of this study is to assess the impact of motion on voxel-based morphometry (VBM) based BAG.

Methods: Data were obtained from two sources: i) T1-weighted (T1w) MRIs from the Cambridge Centre for Ageing and Neuroscience (CamCAN) were used to train the brain age prediction model, and ii) T1w MRIs from the Movement-related artifacts (MR-ART) dataset were used to assess the impact of motion on BAG. MR-ART includes one motion-free and two motion-affected (one low and one high) 3D T1w MRIs. We also visually rated the motion levels of the MR-ART MRIs from 0 to 5, with 0 meaning no motion and 5 high motion levels. All images were pre-processed through a standard VBM pipeline. GM density across cortical and subcortical regions were then used to train the brain age prediction model and assess the relationship between BAG and MRI motion. Principal component analysis was used to perform dimension reduction and extract the VBM-based features. BAG was estimated by regressing out the portion of delta age explained by chronological age. Linear mixed effects models were used to investigate the relationship between BAG and motion session as well as motion severity, including participant IDs as random effects.

Results: In contrast with the session with no induced motion, predicted delta age was significantly higher for high motion sessions (t-value = 5.06, $p < 0.0001$), with marginal effect for low motion sessions (t-value = 1.95, $p = 0.051$). In addition, delta age was significantly associated with motion severity as evaluated by visual rating ($t = 4.46$, $p < 0.0001$).

Conclusion: Motion in the scanner can significantly impact brain age estimates, and needs to be accounted for as a confound, particularly when studying populations that are known to have higher levels of motion in the scanner. These results have significant implications for brain age studies in aging and neurodegeneration. Based on these findings, we recommend assessment and inclusion of visual motion ratings in such studies.

Keywords: brain age, motion, voxel-based morphometry, magnetic resonance imaging

Introduction

Brain aging is a heterogeneous process characterized by morphological and functional brain alterations, resulting in behavioral changes across lifespan (Yankner et al., 2008). These changes are commonly observed in the aging population and are distinct from their counterparts in neurodegenerative disorders. However, aging is also the primary risk factor for most neurodegenerative disorders, including Parkinson's disease (PD) and Alzheimer's disease (AD) (Collier et al., 2011; Hou et al., 2019). As such, the study of aging-related brain changes has been of interest, to develop a baseline characteristic against which abnormal brain alterations can be identified (Bethlehem et al., 2022; Kaufmann et al., 2019a). Similarly, at the individual level, brain aging profile has been proposed as a biomarker for brain health (Franke and Gaser, 2019).

Neuroimaging techniques have been used to study the brain structural changes throughout lifespan. In particular, T1-weighted (T1w) Magnetic resonance imaging (MRI) is widely used in research and clinical settings to study different aspects of brain morphology and its longitudinal changes in a non-invasive manner. Using MRI to investigate brain structure, function, and its abnormalities at high spatial resolution has become a prominent part of the clinical diagnostic routine (Lerch et al., 2017; Rocca et al., 2017; Rüber et al., 2018; Scheltens et al., 2021). Neuroimaging studies of normal brain aging have generated an extensive body of literature regarding the trajectories of the aging brain (Bethlehem et al., 2022; Ferreira and Busatto, 2013; Fjell et al., 2014; Lockhart and DeCarli, 2014). In addition, the need for a valid biomarker of brain aging over the lifespan has been emphasized due to the increasingly recognized importance of interventions to prevent aging related disorders such as AD (Belsky et al., 2015; Elliott et al., 2021).

Due to the individual differences in aging processes (i.e. trajectory and rates across the population as well as throughout the lifespan), biological age, that is, estimated age of a sample, and its offset in comparison with chronological age have been widely used as measures reflecting an individual's healthy or unhealthy aging (Belsky et al., 2015; Elliott et al., 2021; Ferrucci and Kuchel, 2021; Rivero-Segura et al., 2020; Wu et al., 2021). Concerning the brain, this offset, or "Brain Age Gap" (BAG) is defined as the difference between the brain's predicted age and the chronological age of an individual. BAG can be measured using neuroimaging data alongside machine learning models to predict the age of the participants in a healthy aging population (training data). The model is then applied to the population of interest (test data) to calculate BAG and perform group comparisons or assess relationships with phenotypes of interest. BAG can quantify acceleration of brain aging, and is used to measure brain health as aging and disease interact (Cole and Franke, 2017; Franke and Gaser, 2019, 2019). BAG has proven sensitive to various neurological and neuropsychiatric conditions, not only from the spectrum of dementia in late-life, but also in much younger patients with multiple sclerosis (Høgestøl et al., 2019), schizophrenia (Nenadić et al., 2017), obesity (Zeighami et al., 2022), first episode psychosis (Kolenic et al., 2018), diabetes (Franke et al., 2013), gestational Age

(Luders et al., 2018), MCI (Franke and Gaser, 2012), traumatic brain injury (Cole et al., 2015), HIV (Cole et al., 2017b), epilepsy (Pardoe et al., 2017), and Down syndrome (Cole et al., 2017a). BAG has also been used to track brain health improvement in several intervention studies including the effect of bariatric surgery and exercise on brain health.

Previous studies have indirectly shown that head motion is associated with alterations in T1w structural brain measure estimations. As such, head motion may also impact the observed age-related differences. Motion in the scanner is a common occurrence that can affect the acquired MRI data and act as a major confound in MRI-derived models. Motion levels are significantly higher in the older populations as well as in individuals with obesity, PD, and other neurodegenerative disorders. However, the relationship between head motion and BAG has not been directly examined (Kaufmann et al., 2019b; Madan, 2018; Savalia et al., 2017; Wang et al., 2019). The aim of this study is to assess the impact of motion on voxel-based morphometry (VBM) based BAG and evaluate whether including motion as a confounding factor (i.e. as estimated motion ratings) in brain age estimation models would sufficiently account for this confound and improve the accuracy and validity of the findings. Our findings can contribute to the understanding of the relationship between motion and brain age estimations and provide insights into the potential implications of motion in brain age studies, particularly in the usage of BAG in study of aging and neurodegenerative disorders.

Methods

2.1. Data

Data were obtained from two different sources to train the brain age prediction model and evaluate the influence of motion on brain age predictions. These distinct sources served the following purposes: 1) training the brain age prediction model, 2) investigating the potential impact of motion on the BAG.

2.1.1. Training Data

The brain age prediction model was trained using data from participants in the second stage of the Cambridge Centre for Ageing and Neuroscience (CamCAN, https://www.cam-can.org/index.php?content=dataset) dataset (Taylor et al., 2017). Participants with neurological and psychiatric conditions were excluded from the study. The training data was matched with the testing dataset and only included CamCAN participants who passed QC with ages below 50 years. A total of 281 (148 female) were included in the analysis, with age range between 18 and 50 (and mean +/- std of 36.14 +/- 8.6 years). T1-weighted MRIs were acquired on a 3T Siemens TIM Trio, with a 32-channel head-coil using a 3D magnetization-prepared rapid gradient echo (MPRAGE) sequence (TR = 2250 ms, TE = 2.99 ms, TI = 900 ms, FA = 9 deg, field of view (FOV) = 256 × 240 × 192 mm, 1 mm3 isotropic, GRAPPA = 2, TA = 4 min 32 s). For detailed acquisition parameters see: https://camcan-archive.mrc-cbu.cam.ac.uk/dataaccess/pdfs/CAMCAN700_MR_params.pdf.

2.1.2. Movement-related artifacts (MR-ART) dataset

The independent out-of-sample dataset used to assess the impact of motion on BAG comes from a longitudinal investigation aimed at enhancing the understanding of motion artifacts and providing a valuable resource for evaluating and improving existing motion correction techniques (Nárai et al., 2022). The dataset comprises brain scans from 148 healthy participants, the pipeline failed for one subject, we used 434 sessions from the 147 remaining subjects (7 sessions missing). Furthermore, 27 sessions failed the QC for brain mask, linear, or nonlinear registration. The remaining data comprised 127 subjects with all three sessions included (subjects with QC fails for any of the sessions were completely removed). Due to the low number of participants with ages over 50 and a gap in the age distribution in the remaining sample we also removed 6 subjects with ages over 50. The final sample includes 121 subjects, 77 females and 44 males, aged 26.17 ± 6.32 years. None of the participants had a reported history of neurological or psychiatric diseases. Brain scans were performed using a Siemens Magnetom Prisma 3T MRI scanner with a 20-channel head-neck receiver coil at the Brain Imaging Centre. T1-weighted 3D magnetization-prepared rapid gradient echo (MPRAGE) anatomical images were acquired with 2-fold in-plane GRAPPA acceleration and a 1 mm^3 spatial resolution. The scans involved three conditions for each participant: a standard scan (STAND) without motion, a low head motion scan (HM1), and a high head motion scan (HM2). Participants focused on a fixation point during the scans and nodded their heads in response to the word "MOVE" on the screen for HM1 and HM2 scans.

2.2. Quality Control (QC) and Motion Assessment

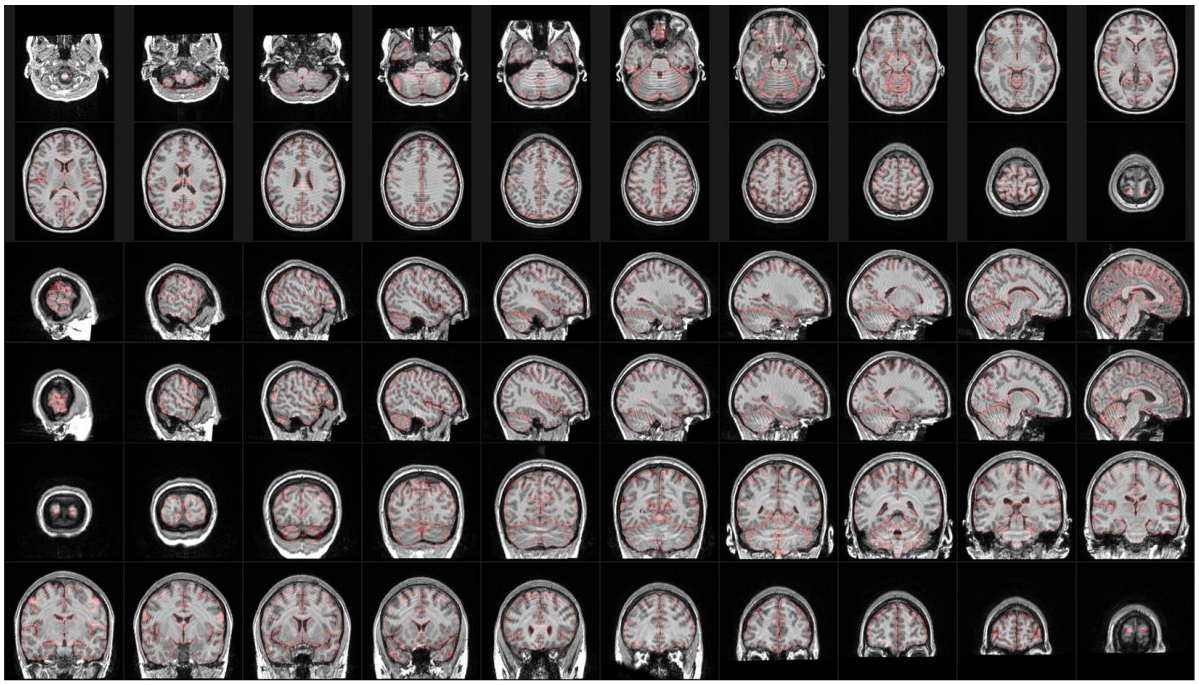

Figure 1. Example QC images showing sagittal, coronal, and axial slices covering the entire brain, used for visual assessment of motion severity.

2.2.1. QC Protocol

For T1w data, the QC protocol involved the following main steps: assessment of presence of artifacts other than motion (e.g. missing slices, incomplete field of view), as well as linear and nonlinear alignment of the images with the outline of the MNI-ICBM152-2009c average template. Registration QC was conducted following the protocols outlined in Dadar et al. 2018, 2022 (Dadar et al., 2022, 2018). Each image in the three datasets underwent these steps, and quality ratings were recorded.

2.2.2. Motion Rating: Visual Inspection and Rating Scale

Every image within the CAMCAN, MR-ART datasets that passed the QC steps outlined in section 2.2.1 underwent a thorough visual inspection process to assess presence and severity of motion (RM). The QC images included sagittal, coronal, and axial slices covering the entire brain, allowing for reliable visualization of motion across the entire scan (see Figure 1 for an example).

The expert rater evaluated each image, assigning a motion score based on a 6-point scale. The scale ranged from 0, indicating no motion, to 5, indicating high levels of motion. The motion level ratings were assigned in increments of 1 to provide a more detailed assessment of motion artifacts present in the images. This meticulous process ensured the accuracy and reliability of the datasets for further analysis and research purposes. Figure 2.A shows representative examples of cases with motion ratings ranging from 0-5. RM repeated the rating process a second time, 6 months after performing the initial ratings and blind to the initial scores, to allow for assessment of intra-rater reliability in motion ratings (Figure 2.B).

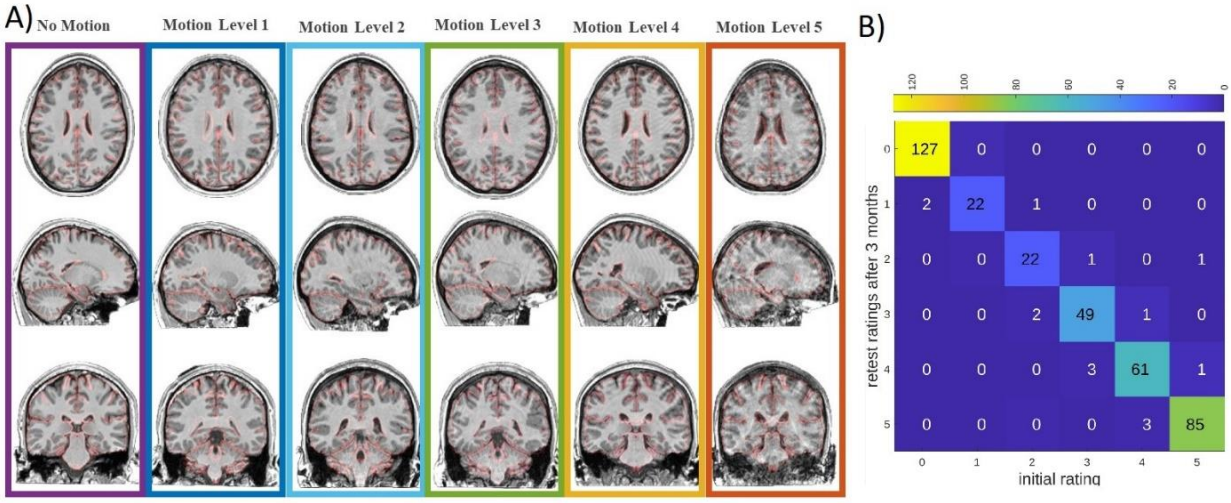

Figure 2. A) Representative examples of cases with no motion (rating: 0) to high motion (rating: 5) based on visual assessment. B) intra-rater agreement for visual rating of motion in MR-ART dataset.

2.3. Voxel-based morphometry

To train the brain age prediction model and investigate the association between predicted brain age and motion, VBM was employed to estimate gray matter density in cortical and subcortical regions. The T1w structural scans underwent a standard VBM pipeline using the following steps: 1) image denoising (Coupé et al., 2008); 2) intensity non-uniformity correction (Sled et al., 1998); and 3) image intensity normalization into range (0–100) using histogram matching. Linear registration to an average brain template (MNI ICBM152–2009c) was performed using a nine-parameter registration (Dadar et al., 2018; Manera et al., 2020), followed by a nonlinear registration using the Advanced Normalization Tools (ANTS) software (Avants et al., 2009). Segmentation of the T1w images into gray matter, white matter, and cerebrospinal fluid was performed using the ANIMAL software (Collins and Evans, 1997). Finally, VBM gray matter density maps per voxel were generated using MNI MINC tools by VBM analysis ("BIC-MNI Software repository," n.d.).

2.4. Brain Age Prediction Model

To predict brain age, similar to our previous works (Zeighami et al., 2022; Zeighami and Evans, 2021) and similar works in the literature (Franke and Gaser, 2019; Lewis et al., 2018; Peng et al., 2021; Smith et al., 2020, 2019), a linear regression model was employed using VBM measures as features, following principal component analysis (PCA) for dimensionality reduction. PCA is a data factorization method based on singular value decomposition that has frequently been employed in studies focused on brain age prediction. To ensure the model's generalizability and prevent overfitting, we employed 10-fold cross-validation. The prediction accuracy obtained from the 10-fold cross-validation was utilized to evaluate the model's performance on the training sample (i.e. CamCAN dataset). It also assisted in determining the optimal number of features to include in the final model. For the linear regression model, the root-mean-squared error (RMSE) was employed as the natural cost function. Finally, two other brain age prediction models were also trained based on the STAND (without motion) and HM2 (high motion) MR-ART sessions, to investigate i) within dataset impact of motion on brain age predictions as well as ii) the effect of using motion-impacted data for training brain age predictions models.

2.5. Assessing the Relationship between BAG and Motion Severity

Once the brain age was predicted as described earlier, we computed the BAG, which represents the difference between the predicted brain age and the chronological age. BAG serves as an indicator of brain-related health, as it quantifies the gap between the brain age estimated from gray matter density and the expected brain age based on chronological age.

(1) $Y = X * \beta 1 - \delta 1 \rightarrow \delta 1 = X * \beta 1 - Y$

In formula (1), $\delta 1$, X, $\beta 1$, and Y indicate BAG, VBM-based principal components, the weights estimated by the model, and chronological age, respectively. BAG is inherently correlated with the participants' chronological age, which can act as a confounding factor in the analysis and complicate the differentiation between the effect of chronological age and the additional biological BAG. To address this issue, various adjustments have been proposed in previous studies (Beheshti et al., 2019; Le et al., 2018; Liang et al., 2019; Smith et al., 2019). In this study, we adopt the definition proposed by Smith et al. in 2019, where we regress out the portion of BAG that can be explained by chronological age (as shown in formula (2)) (Smith et al., 2019). The residual after accounting for the influence of chronological age is referred to as the adjusted BAG.

(2) $\delta 2 = \delta 1 - Y * \beta 2$

$\delta 2$ and $\beta 2$ In formula (2), represent the adjusted BAG and the estimated weights by the model, respectively. The adjusted BAG serves as the primary measure of interest in this work.

2.6. Statistical analyses

For the MR-ART dataset, the trained models were utilized to predict brain age for the participants, not accounting for the presence of motion artifacts in this dataset. The model used for prediction was trained on the CamCAN dataset. This allowed us to assess the effect of motion artifacts on the BAG within this dataset. Following the predictions, we calculated the adjusted BAG for the test sample. Two sets of linear mixed effects models were used to assess whether presence of motion impacted the adjusted BAG estimates, one with session (contrasting the sessions with motion against the session without motion) as a categorical variable of interest contrasting the two sessions with motion (HM1 and HM2) against the session without motion (STAND), and another with the motion scores as a continuous variable of interest. All models included participant ID as a categorical random effect.

(1) Adjusted BAG ~ motion session + (1|ID)
(2) Adjusted BAG ~ visual motion rating + (1|ID)

We also evaluated the effect of motion across brain age prediction features. To do so we used the first 45 principal component (PC) maps derived from the training dataset and included in the prediction model. These PCs were projected to the MR-ART data normalized based on the CamCAN dataset (as was done for brain age prediction analysis). These projections were then used in linear mixed-effect models to evaluate whether there is any main effect of motion session (both low and high session) as well as the visual motion rating on the MR-ART projection of PCs. The results were then corrected for multiple comparisons using false discovery rate (FDR) correction based on Benjamini-Hochberg.

(3) MR-ART subjects' weight from principal component (i) ~ motion session + (1|ID)
(4) MR-ART subjects' weight from principal component (i) ~ visual motion rating + (1|ID)

All the prediction and statistical analyses described were performed using MATLAB 2022b.

3. Results

In total, 27 participants were excluded from the MR-ART dataset due to missing data from one of the sessions, failing linear and nonlinear registration, as well as age distribution. Figure 2.b summarizes the intra-rater agreement results for the visual motion ratings in the remaining MR-ART sample, showing excellent intra-rater agreement across the two rating sessions. Figure 3 shows the correspondence between MR-ART motion sessions and visual motion ratings (Figure 3.B), as well as examples of scans with different visual motion scores within the same MR-ART motion session (Figure 3.A).

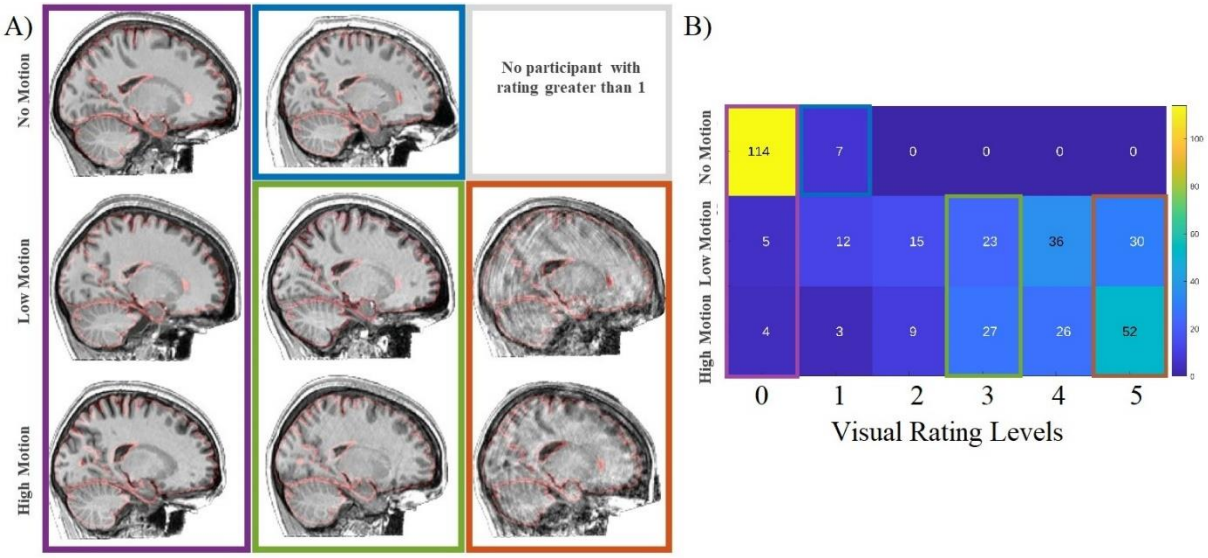

Figure 3. A) Correspondence between session and visual rating. Purple box shows example cases with motion rating values of 0 across the three motion sessions. Blue shows an example of a case with level 1 motion in the no-motion session (there were no higher motion ratings in the no-motion session). Green box shows examples of cases with motion level 3 in low and high motion sessions. Orange box shows examples of cases with motion level 5 in low and high motion sessions. B) Numerical values for number of overlapping cases across session and visual ratings.

3.1. Brain age prediction model

Using the linear regression model trained based on the principal components of the gray matter VBM, it was possible to predict the chronological age of the CamCAN dataset with a correlation of $r = 0.8$ ($p<0.0001$), cross-validated RMSE of 4.1 for adjusted BAG and 5.2 for BAG. The age prediction model was evaluated based on the number of the principal components included in the training dataset, which is the result of 10-fold cross validation and using RMSE as the cost function for age prediction. We determined the optimal number of principal components by selecting the value that yielded the lowest RMSE ($N = 45$). Consequently, our predictive

models rely on 45 VBM-based principal components as the key features for prediction. In order to calculate the features for the analysis, the principal components were projected to the out-of-sample MR-ART dataset.

Boxplots of adjusted BAGs for each motion session in the MR-ART dataset are illustrated in Figure 4.A. In sessions where motion was induced, we found that the predicted delta age was significantly higher compared to sessions without induced motion. This was observed in both the low-motion and high-motion sessions, as demonstrated by the respective beta values of 0.9 years ($t = 1.95$, $p=0.051$) and 2.33 years ($t = 5.06$, $p < 0.0001$). These findings highlight the adverse impact of induced motion on the estimation of delta age, suggesting that motion can considerably influence the assessment of brain health.

Furthermore, we explored the relationship between motion severity (as assessed through visual ratings) and BAG. The results showed a significant association between motion severity and BAG, further highlighting the relationship between motion artifacts and the estimated age-related brain changes. Specifically, we observed that for every unit increase in motion rate as assessed by the visual rating, the estimated delta age increased by 0.45 years ($t = 4.46$, $p < 0.0001$). These findings highlight the critical importance of considering and accounting for motion artifacts when interpreting delta age estimates. Figure 4.B visually represents these findings.

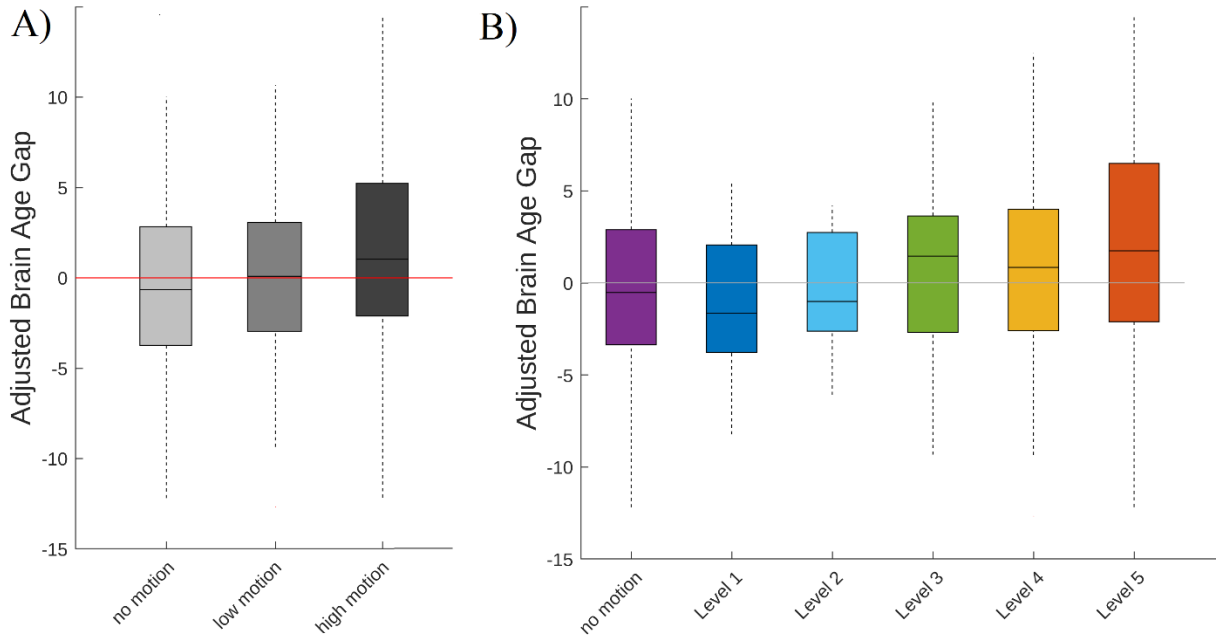

Figure 4. A) Adjusted brain age gap across sessions. B) Adjusted brain age gap across visual motion rating levels.

Finally, as another validation step, we trained the brain age prediction model with cross-validation on the no motion session, and applied it to data from low and high motion sessions,

yielding similar results. In comparison with the STAND session with no motion, there was a significant increase in the adjusted BAG in both low ($t = 2.24$, $p = 0.025$) and high ($t = 6.93$, $p < 0.0001$) motion sessions. Similarly, we observed a significant increase in the adjusted BAG for higher motion severity as assessed by the visual ratings ($t = 5.94$, $p < 0.0001$). We also repeated this analysis a second time, training on high motion data and testing on the entire dataset. The results were very similar for adjusted BAG between no motion and high motion sessions ($t = 5.49$, $p < 0.0001$) as well as the relationship between adjusted BAG and the visual motion ratings ($t = 4.33$, $p < 0.0001$), but no significant differences were found between no motion and low motion sessions ($t = 1.14$, $p > 0.05$).

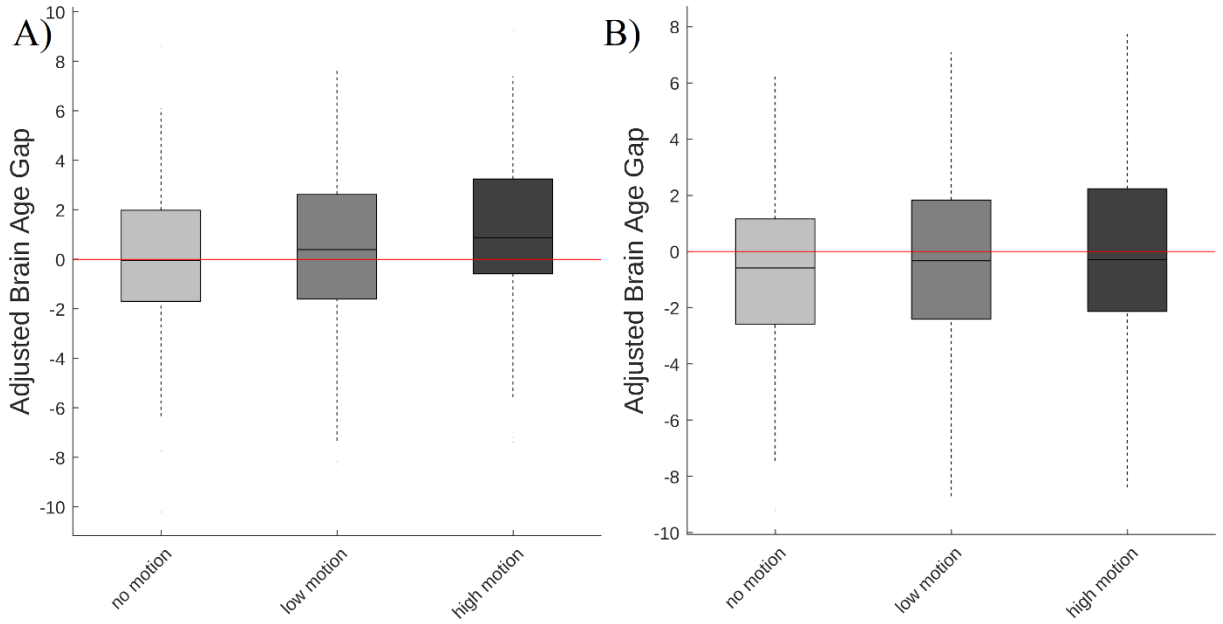

Figure 5. A) Adjusted brain age gap trained on the no-motion (STAND) session with cross validation, applied to all sessions. B) Adjusted brain age gap trained on the high-motion (HM2) session with cross validation and applied to all sessions.

In order to evaluate the effect of motion across brain age prediction features, we ran similar mixed-effect models to evaluate whether there is any main effect of motion session (both low and high session) as well as the visual motion rating on the predictive features These features are the first 45 PC maps derived from the training dataset and included in the prediction model and further projected to the MR-ART data normalized based on training data. While evaluating the effect of sessions we found significant difference after FDR correction between low motion session and no motion in 22 PCs (out of 45 PCs included, explaining 27% of the total variance in CamCAN data) and between high motion and no motion in 36 PCs (out of 45 PCs included, explaining 40% of the total variance in CamCAN data). The results for visually rated motion were very similar to the high motion session with 35 PCs showing significant relationship with motion levels after FDR correction (out of 45 PCs included, explaining 39% of the total variance

in CamCAN data). The only differences between the two models were in PCs number 16, 23, and 10, The first two (i.e., PC-16 and PC-23 both showed significant difference between high and no motion but not a significant relationship with visual rating and PC-10 vice versa). We have shown the z-scored pattern of the first 4 PCs here as an example of the main patterns affected in both models. The information for the t-values and p-values of the models and the brain patterns can be found in our supplementary materials.

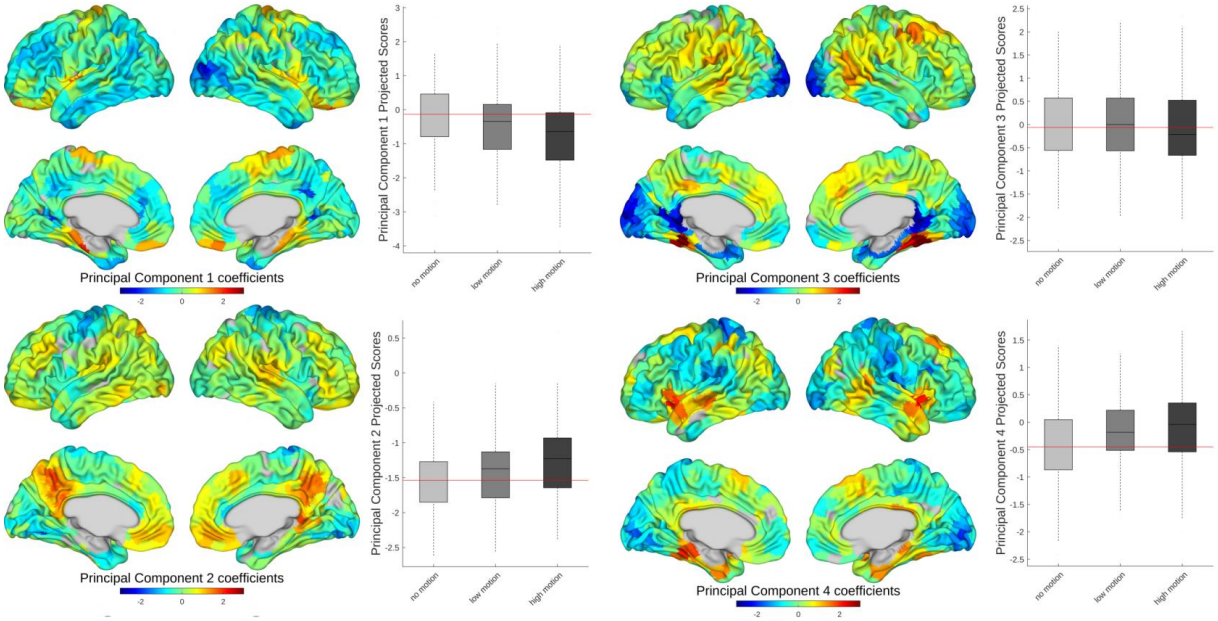

Figure 6. The normalized maps of the first 4 principal components used in age prediction. All four principal components are significantly different between no-motion and high-motion sessions after FDR correction. Each principal component map is accompanied by a boxplot for its corresponding scores for each MR-ART data point across three sessions.

Discussion

In this work, we evaluated the influence of head motion on BAG estimation, determined by changes in brain age prediction derived from VBM measurements. Analyzing the independent MR-ART dataset, we observed that the same individuals rescanned with head motion induced during scanning exhibited significantly greater BAGs. Our study demonstrated a robust correlation between the prediction of BAG changes and the three motion levels of the MR-ART dataset. When compared to the session with no induced motion, the low-motion session exhibited a significantly higher brain age gap, with an average increase of 0.90 years, while the high-motion session showed an even greater increase, with an average of 2.33 years. These results were further validated through motion level ratings assessed visually by an expert, where the results revealed a notable systematic change in the BAG, as evidenced by an average

increase of 0.44 years per level of visually rated motion from 0 to 5, approximately 1.5 to 2 years for high motion levels.

BAG is a widely used measure of brain health that allows for assessment of individual age-related brain changes, providing a personalized biomarker of brain health. BAG can be used to determine biological aging, predict rate of aging, and to monitor the fundamental processes of aging accurately, efficiently, and non-invasively. Furthermore, BAG can be used to assess and quantify accelerations in brain changes due to various brain disorders. While biomarkers that are closely tied to the mechanistic aging process are preferable, structural MRI-based BAG estimations offer higher correlations to age and diagnostic specificity. Hence, BAG provides a more practical and effective approach for assessing and tracking individual brain aging trajectories over time. As such, numerous recent studies have employed BAG estimates as biomarkers of brain health.

As a biomarker, BAG has provided a reference for age-related alterations in brain structure. Moreover, it has demonstrated significant potential for convenient implementation in multi-center studies. The significant predictive accuracy obtained from assessing the structural and functional brain age could be instrumental in tailoring personalized neuroprotective treatments and interventions. It has been shown that late-life cognitive decline can be predicted in patients with mild cognitive impairment and AD based on the brain age gap. Furthermore, research indicates that a higher brain age gap during midlife is preceded by a decline in cognitive functioning that begins in childhood and continues over time. Although it may be intuitive to associate a higher brain age gap with unhealthy lifestyle choices, such as smoking or alcohol consumption, and subsequent cognitive decline, our findings indicate that the predicted increase in BAG can also be influenced by motion artifacts (Franke and Gaser, 2012; Elliott et al., 2021).

The impact of head motion on structural and functional brain measure estimations has been well-documented in previous studies. Head motion, a common occurrence during MRI scanning, has the potential to significantly affect MRI data and act as a major confounding factor in MRI-derived models. These effects include but are not limited to a reduction in gray matter volume as well as blurring between the cortical gray and white matter boundaries and consequently change in cortical thickness (Alexander-Bloch et al., 2016; Bedford et al., 2020; Pardoe et al., 2016; Reuter et al., 2015). Given the negative association of age with brain volume and cortical thickness, both of these effects will result in higher age estimation and consequently higher BAGs. Motion levels are also higher in older populations and particularly in individuals with obesity, PD, and other neurodegenerative disorders. Therefore, systematic biases in the estimated BAGs in these populations can confound the biologically relevant portions of BAG. Therefore, it is crucial to address and account for head motion effects when interpreting age-related differences in brain measures. However, the relationship between head motion and BAG has not been directly examined (Pujol et al., 2014; Reuter et al., 2015). Our results provide a systematic approach to quantify these effects as well as an estimate for the effect size of this given bias for a given motion level. Furthermore, we have made our motion ratings for the open

access MR-ART datasets publicly available (Supplementary Table 1), which can help other researchers estimate and remove motion-related confounding factors from their studies.

Our study benefits from several strengths that enhance the robustness and reliability of our findings. Firstly, we conducted training and validation on different datasets, ensuring the generalizability of our results beyond the specific dataset used for training. This approach enhances the validity of our conclusions and allows for a more comprehensive assessment of the predictive accuracy of our models. Secondly, our study used a validation dataset comprising scans from the same individuals scanned three times with different motion levels, enabling direct comparisons of brain age estimates based on motion within the same subject. This internal validation provides a rigorous assessment of our models and preprocessing methods, adding further credibility to our findings.

The image acquisition method in MR-ART datasets was designed to encompass three levels of motion for each subject, ranging from no motion to a high level of motion. It is important to note that the levels of motion were closely related to human actions; hence, the three motion labels did not precisely represent distinct categories within these specified levels of motion. Consequently, during expert evaluation, the datasets were effectively categorized into six distinct levels of motion, to provide more accurate measurements of the severity of motion occurring in each image, as not all participants had exhibited the same level of motion in each session. BAGs showed an even stronger relationship with motion severity ratings, further supporting our results.

Our study is not without limitations. Firstly, our sample from MR-ART consisted only of healthy participants from a relatively limited age range, which may limit the generalizability of our findings to more vulnerable population groups or people in later life stages. Utilizing more diverse and heterogeneous samples could enhance our ability to identify the impact of motion on the BAG. Secondly, the motion dataset did not include behavioral measures that could have provided valuable insights into differences in the relationships between motion-impacted BAG and cognitive scores. The absence of such data restricts our ability to fully explore the potential links between motion artifacts and the brain estimates of cognitive outcomes. Additionally, the motion dataset may not be fully representative of natural motion occurring in the scanner or motion associated with specific diseases like PD. The patterns of motion observed in the dataset might not entirely mirror the natural motion experienced by individuals during brain imaging scans, which can introduce potential biases in our analysis. Furthermore, here we are using a rather simple model for brain age prediction. While we compared our model with other methods such as support vector machines and found very similar results and no change in performance or conclusions, future studies using more advanced methods such as deep neural network models for age prediction might further improve the prediction performance and the motion bias estimation. Finally, future studies are needed to simulate natural motion artifacts and provide solutions for robust motion removal that can recover the brain age estimates based on the no motion data from these motion contaminated scans.

In conclusion, we showed that participants' motion in the scanner during acquisition of T1w images can significantly and systematically impact the derived BAG estimates. Our results suggest that brain age studies would benefit from considering assessment of motion severity, particularly visual rating of the input scans and potentially including motion severity as a covariate in the models.

Acknowledgements

Data for the training dataset was obtained from the Cambridge Centre for Ageing and Neuroscience (CamCAN). CamCAN funding was provided by the UK Biotechnology and Biological Sciences Research Council (grant number BB/H008217/1), together with support from the UK Medical Research Council and University of Cambridge, UK. HCP data was obtained from the Human Connectome Project, WU-Minn Consortium (Principal Investigators: David Van Essen and Kamil Ugurbil; 1U54MH091657) funded by the 16 NIH Institutes and Centers that support the NIH Blueprint for Neuroscience Research; and by the McDonnell Centre for Systems Neuroscience at Washington University. Authors thank Compute Canada (https://www.computecanada.ca/home) for the usage of the computing resources in the current work.

Funding

Dr. Zeighami reports receiving research funding from the Healthy Brains for Healthy Lives, Fonds de recherche du Québec – Santé (FRQS) Chercheurs boursiers et chercheuses boursières en Intelligence artificielle, as well as Natural Sciences and Engineering Research (NSERC) discovery grant. Dr. Dadar reports receiving research funding from the Healthy Brains for Healthy Lives, NSERC, FRQS, and the Douglas Research Centre (DRC).

References

Alexander-Bloch, A., Clasen, L., Stockman, M., Ronan, L., Lalonde, F., Giedd, J., Raznahan, A., 2016. Subtle in-scanner motion biases automated measurement of brain anatomy from in vivo MRI. Hum. Brain Mapp. 37, 2385–2397.

Avants, B.B., Tustison, N., Song, G., 2009. Advanced normalization tools (ANTS). Insight J 2, 1–35.

Bedford, S.A., Park, M.T.M., Devenyi, G.A., Tullo, S., Germann, J., Patel, R., Anagnostou, E., Baron-Cohen, S., Bullmore, E.T., Chura, L.R., Craig, M.C., Ecker, C., Floris, D.L., Holt, R.J., Lenroot, R., Lerch, J.P., Lombardo, M.V., Murphy, D.G.M., Raznahan, A., Ruigrok, A.N.V., Smith, E., Spencer, M.D., Suckling, J., Taylor, M.J., Thurm, A., Lai, M.-C., Chakravarty, M.M., 2020. Large-scale analyses of the relationship between sex, age and intelligence quotient heterogeneity and cortical morphometry in autism spectrum disorder. Mol. Psychiatry 25, 614–628. https://doi.org/10.1038/s41380-019-0420-6

Beheshti, I., Nugent, S., Potvin, O., Duchesne, S., 2019. Bias-adjustment in neuroimaging-based brain age frameworks: A robust scheme. NeuroImage Clin. 24, 102063.

Belsky, D.W., Caspi, A., Houts, R., Cohen, H.J., Corcoran, D.L., Danese, A., Harrington, H., Israel, S.,

Levine, M.E., Schaefer, J.D., 2015. Quantification of biological aging in young adults. Proc. Natl. Acad. Sci. 112, E4104–E4110.

Bethlehem, R.A.I., Seidlitz, J., White, S.R., Vogel, J.W., Anderson, K.M., Adamson, C., Adler, S., Alexopoulos, G.S., Anagnostou, E., Areces-Gonzalez, A., Astle, D.E., Auyeung, B., Ayub, M., Bae, J., Ball, G., Baron-Cohen, S., Beare, R., Bedford, S.A., Benegal, V., Beyer, F., Blangero, J., Cábez, M.B., Boardman, J.P., Borzage, M., Bosch-Bayard, J.F., Bourke, N., Calhoun, V.D., Chakravarty, M.M., Chen, C., Chertavian, C., Chetelat, G., Chong, Y.S., Cole, J.H., Corvin, A., Costantino, M., Courchesne, E., Crivello, F., Cropley, V.L., Crosbie, J., Crossley, N., Delarue, M., Delorme, R., Desrivieres, S., Devenyi, G.A., Biase, M.A.D., Dolan, R., Donald, K.A., Donohoe, G., Dunlop, K., Edwards, A.D., Elison, J.T., Ellis, C.T., Elman, J.A., Eyler, L., Fair, D.A., Feczko, E., Fletcher, P.C., Fonagy, P., Franz, C.E., Galan-Garcia, L., Gholipour, A., Giedd, J., Gilmore, J.H., Glahn, D.C., Goodyer, I.M., Grant, P.E., Groenewold, N.A., Gunning, F.M., Gur, R.E., Gur, R.C., Hammill, C.F., Hansson, O., Hedden, T., Heinz, A., Henson, R.N., Heuer, K., Hoare, J., Holla, B., Holmes, A.J., Holt, R., Huang, H., Im, K., Ipser, J., Jack, C.R., Jackowski, A.P., Jia, T., Johnson, K.A., Jones, P.B., Jones, D.T., Kahn, R.S., Karlsson, H., Karlsson, L., Kawashima, R., Kelley, E.A., Kern, S., Kim, K.W., Kitzbichler, M.G., Kremen, W.S., Lalonde, F., Landeau, B., Lee, S., Lerch, J., Lewis, J.D., Li, J., Liao, W., Liston, C., Lombardo, M.V., Lv, J., Lynch, C., Mallard, T.T., Marcelis, M., Markello, R.D., Mathias, S.R., Mazoyer, B., McGuire, P., Meaney, M.J., Mechelli, A., Medic, N., Misic, B., Morgan, S.E., Mothersill, D., Nigg, J., Ong, M.Q.W., Ortinau, C., Ossenkoppele, R., Ouyang, M., Palaniyappan, L., Paly, L., Pan, P.M., Pantelis, C., Park, M.M., Paus, T., Pausova, Z., Paz-Linares, D., Binette, A.P., Pierce, K., Qian, X., Qiu, J., Qiu, A., Raznahan, A., Rittman, T., Rodrigue, A., Rollins, C.K., Romero-Garcia, R., Ronan, L., Rosenberg, M.D., Rowitch, D.H., Salum, G.A., Satterthwaite, T.D., Schaare, H.L., Schachar, R.J., Schultz, A.P., Schumann, G., Schöll, M., Sharp, D., Shinohara, R.T., Skoog, I., Smyser, C.D., Sperling, R.A., Stein, D.J., Stolicyn, A., Suckling, J., Sullivan, G., Taki, Y., Thyreau, B., Toro, R., Traut, N., Tsvetanov, K.A., Turk-Browne, N.B., Tuulari, J.J., Tzourio, C., Vachon-Presseau, É., Valdes-Sosa, M.J., Valdes-Sosa, P.A., Valk, S.L., Amelsvoort, T. van, Vandekar, S.N., Vasung, L., Victoria, L.W., Villeneuve, S., Villringer, A., Vértes, P.E., Wagstyl, K., Wang, Y.S., Warfield, S.K., Warrier, V., Westman, E., Westwater, M.L., Whalley, H.C., Witte, A.V., Yang, N., Yeo, B., Yun, H., Zalesky, A., Zar, H.J., Zettergren, A., Zhou, J.H., Ziauddeen, H., Zugman, A., Zuo, X.N., 3R-BRAIN, Rowe, C., Initiative, A.D.N., Frisoni, G.B., Team, C., Cam-CAN, CCNP, COBRE, cVEDA, Group, E.D.B.A.W., Project, D.H.C., FinnBrain, Study, H.A.B., IMAGEN, KNE96, Aging, T.M.C.S. of, NSPN, POND, Binette, A.P., VETSA, Bullmore, E.T., Alexander-Bloch, A.F., 2022. Brain charts for the human lifespan. Nature 604, 525–533. https://doi.org/10.1038/s41586-022-04554-y

BIC-MNI Software repository [WWW Document], n.d. URL http://bic-mni.github.io/ (accessed 2.12.23).

Cole, J.H., Annus, T., Wilson, L.R., Remtulla, R., Hong, Y.T., Fryer, T.D., Acosta-Cabronero, J., Cardenas-Blanco, A., Smith, R., Menon, D.K., 2017a. Brain-predicted age in Down syndrome is associated with beta amyloid deposition and cognitive decline. Neurobiol. Aging 56, 41–49.

Cole, J.H., Franke, K., 2017. Predicting Age Using Neuroimaging: Innovative Brain Ageing Biomarkers. Trends Neurosci. 40, 681–690. https://doi.org/10.1016/j.tins.2017.10.001

Cole, J.H., Leech, R., Sharp, D.J., Initiative, A.D.N., 2015. Prediction of brain age suggests accelerated atrophy after traumatic brain injury. Ann. Neurol. 77, 571–581.

Cole, J.H., Underwood, J., Caan, M.W., De Francesco, D., van Zoest, R.A., Leech, R., Wit, F.W.,

Portegies, P., Geurtsen, G.J., Schmand, B.A., 2017b. Increased brain-predicted aging in treated HIV disease. Neurology 88, 1349–1357.

Collier, T.J., Kanaan, N.M., Kordower, J.H., 2011. Ageing as a primary risk factor for Parkinson's disease: evidence from studies of non-human primates. Nat. Rev. Neurosci. 12, 359–366. https://doi.org/10.1038/nrn3039

Collins, D.L., Evans, A.C., 1997. Animal: validation and applications of nonlinear registration-based segmentation. Int. J. Pattern Recognit. Artif. Intell. 11, 1271–1294.

Coupé, P., Yger, P., Prima, S., Hellier, P., Kervrann, C., Barillot, C., 2008. An optimized blockwise nonlocal means denoising filter for 3-D magnetic resonance images. IEEE Trans. Med. Imaging 27, 425–441.

Dadar, M., Camicioli, R., Duchesne, S., 2022. Multi sequence average templates for aging and neurodegenerative disease populations. Sci. Data 9, 1–13.

Dadar, M., Fonov, V.S., Collins, D.L., Initiative, A.D.N., 2018. A comparison of publicly available linear MRI stereotaxic registration techniques. Neuroimage 174, 191–200.

Elliott, M.L., Belsky, D.W., Knodt, A.R., Ireland, D., Melzer, T.R., Poulton, R., Ramrakha, S., Caspi, A., Moffitt, T.E., Hariri, A.R., 2021. Brain-age in midlife is associated with accelerated biological aging and cognitive decline in a longitudinal birth cohort. Mol. Psychiatry 26, 3829–3838.

Ferreira, L.K., Busatto, G.F., 2013. Resting-state functional connectivity in normal brain aging. Neurosci. Biobehav. Rev. 37, 384–400.

Ferrucci, L., Kuchel, G.A., 2021. Heterogeneity of aging: individual risk factors, mechanisms, patient priorities, and outcomes. J. Am. Geriatr. Soc. 69, 610.

Fjell, A.M., McEvoy, L., Holland, D., Dale, A.M., Walhovd, K.B., Initiative, A.D.N., 2014. What is normal in normal aging? Effects of aging, amyloid and Alzheimer's disease on the cerebral cortex and the hippocampus. Prog. Neurobiol. 117, 20–40.

Franke, K., Gaser, C., 2019. Ten Years of BrainAGE as a Neuroimaging Biomarker of Brain Aging: What Insights Have We Gained? Front. Neurol. 10.

Franke, K., Gaser, C., 2012. Longitudinal changes in individual BrainAGE in healthy aging, mild cognitive impairment, and Alzheimer's disease. GeroPsych.

Franke, K., Gaser, C., Manor, B., Novak, V., 2013. Advanced BrainAGE in older adults with type 2 diabetes mellitus. Front. Aging Neurosci. 5, 90.

Høgestøl, E.A., Kaufmann, T., Nygaard, G.O., Beyer, M.K., Sowa, P., Nordvik, J.E., Kolskår, K., Richard, G., Andreassen, O.A., Harbo, H.F., Westlye, L.T., 2019. Cross-Sectional and Longitudinal MRI Brain Scans Reveal Accelerated Brain Aging in Multiple Sclerosis. Front. Neurol. 10.

Hou, Y., Dan, X., Babbar, M., Wei, Y., Hasselbalch, S.G., Croteau, D.L., Bohr, V.A., 2019. Ageing as a risk factor for neurodegenerative disease. Nat. Rev. Neurol. 15, 565–581. https://doi.org/10.1038/s41582-019-0244-7

Kaufmann, T., Meer, D. van der, Doan, N.T., Schwarz, E., Lund, M.J., Agartz, I., Alnæs, D., Barch,

D.M., Baur-Streubel, R., Bertolino, A., Bettella, F., Beyer, M.K., Bøen, E., Borgwardt, S., Brandt, C.L., Buitelaar, J., Celius, E.G., Cervenka, S., Conzelmann, A., Córdova-Palomera, A., Dale, A.M., Quervain, D.J.F. de, Carlo, P.D., Djurovic, S., Dørum, E.S., Eisenacher, S., Elvsåshagen, T., Espeseth, T., Fatouros-Bergman, H., Flyckt, L., Franke, B., Frei, O., Haatveit, B., Håberg, A.K., Harbo, H.F., Hartman, C.A., Heslenfeld, D., Hoekstra, P.J., Høgestøl, E.A., Jernigan, T.L., Jonassen, R., Jönsson, E.G., Farde, L., Flyckt, L., Engberg, G., Erhardt, S., Fatouros-Bergman, H., Cervenka, S., Schwieler, L., Piehl, F., Agartz, I., Collste, K., Victorsson, P., Malmqvist, A., Hedberg, M., Orhan, F., Kirsch, P., Kłoszewska, I., Kolskår, K.K., Landrø, N.I., Hellard, S.L., Lesch, K.-P., Lovestone, S., Lundervold, A., Lundervold, A.J., Maglanoc, L.A., Malt, U.F., Mecocci, P., Melle, I., Meyer-Lindenberg, A., Moberget, T., Norbom, L.B., Nordvik, J.E., Nyberg, L., Oosterlaan, J., Papalino, M., Papassotiropoulos, A., Pauli, P., Pergola, G., Persson, K., Richard, G., Rokicki, J., Sanders, A.-M., Selbæk, G., Shadrin, A.A., Smeland, O.B., Soininen, H., Sowa, P., Steen, V.M., Tsolaki, M., Ulrichsen, K.M., Vellas, B., Wang, L., Westman, E., Ziegler, G.C., Zink, M., Andreassen, O.A., Westlye, L.T., 2019a. Common brain disorders are associated with heritable patterns of apparent aging of the brain. Nat. Neurosci. 22, 1617–1623. https://doi.org/10.1038/s41593-019-0471-7

Kaufmann, T., van der Meer, D., Doan, N.T., Schwarz, E., Lund, M.J., Agartz, I., Alnæs, D., Barch, D.M., Baur-Streubel, R., Bertolino, A., 2019b. Common brain disorders are associated with heritable patterns of apparent aging of the brain. Nat. Neurosci. 22, 1617–1623.

Kolenic, M., Franke, K., Hlinka, J., Matejka, M., Capkova, J., Pausova, Z., Uher, R., Alda, M., Spaniel, F., Hajek, T., 2018. Obesity, dyslipidemia and brain age in first-episode psychosis. J. Psychiatr. Res. 99, 151–158.

Le, T.T., Kuplicki, R.T., McKinney, B.A., Yeh, H.-W., Thompson, W.K., Paulus, M.P., Investigators, T. 1000, 2018. A nonlinear simulation framework supports adjusting for age when analyzing BrainAGE. Front. Aging Neurosci. 10, 317.

Lerch, J.P., Van Der Kouwe, A.J., Raznahan, A., Paus, T., Johansen-Berg, H., Miller, K.L., Smith, S.M., Fischl, B., Sotiropoulos, S.N., 2017. Studying neuroanatomy using MRI. Nat. Neurosci. 20, 314–326.

Lewis, J.D., Evans, A.C., Tohka, J., Group, B.D.C., 2018. T1 white/gray contrast as a predictor of chronological age, and an index of cognitive performance. Neuroimage 173, 341–350.

Liang, H., Zhang, F., Niu, X., 2019. Investigating systematic bias in brain age estimation with application to post-traumatic stress disorders. Wiley Online Library.

Lockhart, S.N., DeCarli, C., 2014. Structural imaging measures of brain aging. Neuropsychol. Rev. 24, 271–289.

Luders, E., Gingnell, M., Poromaa, I.S., Engman, J., Kurth, F., Gaser, C., 2018. Potential brain age reversal after pregnancy: younger brains at 4–6 weeks postpartum. Neuroscience 386, 309–314.

Madan, C.R., 2018. Age differences in head motion and estimates of cortical morphology. PeerJ 6, e5176.

Manera, A.L., Dadar, M., Fonov, V., Collins, D.L., 2020. CerebrA, registration and manual label correction of Mindboggle-101 atlas for MNI-ICBM152 template. Sci. Data 7, 237. https://doi.org/10.1038/s41597-020-0557-9

Nárai, Á., Hermann, P., Auer, T., Kemenczky, P., Szalma, J., Homolya, I., Somogyi, E., Vakli, P., Weiss,

B., Vidnyánszky, Z., 2022. Movement-related artefacts (MR-ART) dataset of matched motion-corrupted and clean structural MRI brain scans. Sci. Data 9, 630.

Nenadić, I., Dietzek, M., Langbein, K., Sauer, H., Gaser, C., 2017. BrainAGE score indicates accelerated brain aging in schizophrenia, but not bipolar disorder. Psychiatry Res. Neuroimaging 266, 86–89.

Pardoe, H.R., Cole, J.H., Blackmon, K., Thesen, T., Kuzniecky, R., Investigators, H.E.P., 2017. Structural brain changes in medically refractory focal epilepsy resemble premature brain aging. Epilepsy Res. 133, 28–32.

Pardoe, H.R., Hiess, R.K., Kuzniecky, R., 2016. Motion and morphometry in clinical and nonclinical populations. Neuroimage 135, 177–185.

Peng, H., Gong, W., Beckmann, C.F., Vedaldi, A., Smith, S.M., 2021. Accurate brain age prediction with lightweight deep neural networks. Med. Image Anal. 68, 101871.

Pujol, J., Macià, D., Blanco-Hinojo, L., Martínez-Vilavella, G., Sunyer, J., de la Torre, R., Caixàs, A., Martín-Santos, R., Deus, J., Harrison, B.J., 2014. Does motion-related brain functional connectivity reflect both artifacts and genuine neural activity? NeuroImage 101, 87–95. https://doi.org/10.1016/j.neuroimage.2014.06.065

Reuter, M., Tisdall, M.D., Qureshi, A., Buckner, R.L., van der Kouwe, A.J., Fischl, B., 2015. Head motion during MRI acquisition reduces gray matter volume and thickness estimates. Neuroimage 107, 107–115.

Rivero-Segura, N.A., Bello-Chavolla, O.Y., Barrera-Vázquez, O.S., Gutierrez-Robledo, L.M., Gomez-Verjan, J.C., 2020. Promising biomarkers of human aging: In search of a multi-omics panel to understand the aging process from a multidimensional perspective. Ageing Res. Rev. 64, 101164.

Rocca, M.A., Battaglini, M., Benedict, R.H., De Stefano, N., Geurts, J.J., Henry, R.G., Horsfield, M.A., Jenkinson, M., Pagani, E., Filippi, M., 2017. Brain MRI atrophy quantification in MS: from methods to clinical application. Neurology 88, 403–413.

Rüber, T., David, B., Elger, C.E., 2018. MRI in epilepsy: clinical standard and evolution. Curr. Opin. Neurol. 31, 223–231.

Savalia, N.K., Agres, P.F., Chan, M.Y., Feczko, E.J., Kennedy, K.M., Wig, G.S., 2017. Motion-related artifacts in structural brain images revealed with independent estimates of in-scanner head motion. Hum. Brain Mapp. 38, 472–492.

Scheltens, P., De Strooper, B., Kivipelto, M., Holstege, H., Chételat, G., Teunissen, C.E., Cummings, J., van der Flier, W.M., 2021. Alzheimer's disease. The Lancet 397, 1577–1590.

Sled, J.G., Zijdenbos, A.P., Evans, A.C., 1998. A nonparametric method for automatic correction of intensity nonuniformity in MRI data. IEEE Trans. Med. Imaging 17, 87–97.

Smith, S.M., Elliott, L.T., Alfaro-Almagro, F., McCarthy, P., Nichols, T.E., Douaud, G., Miller, K.L., 2020. Brain aging comprises many modes of structural and functional change with distinct genetic and biophysical associations. Elife 9, e52677.

Smith, S.M., Vidaurre, D., Alfaro-Almagro, F., Nichols, T.E., Miller, K.L., 2019. Estimation of brain age delta from brain imaging. Neuroimage 200, 528–539.

Taylor, J.R., Williams, N., Cusack, R., Auer, T., Shafto, M.A., Dixon, M., Tyler, L.K., Henson, R.N., 2017. The Cambridge Centre for Ageing and Neuroscience (Cam-CAN) data repository: Structural and functional MRI, MEG, and cognitive data from a cross-sectional adult lifespan sample. Neuroimage 144, 262–269.

Wang, J., Knol, M.J., Tiulpin, A., Dubost, F., de Bruijne, M., Vernooij, M.W., Adams, H.H., Ikram, M.A., Niessen, W.J., Roshchupkin, G.V., 2019. Gray matter age prediction as a biomarker for risk of dementia. Proc. Natl. Acad. Sci. 116, 21213–21218.

Wu, J.W., Yaqub, A., Ma, Y., Koudstaal, W., Hofman, A., Ikram, M.A., Ghanbari, M., Goudsmit, J., 2021. Biological age in healthy elderly predicts aging-related diseases including dementia. Sci. Rep. 11, 15929.

Yankner, B.A., Lu, T., Loerch, P., 2008. The aging brain. Annu Rev Pathol Mech Dis 3, 41–66.

Zeighami, Y., Dadar, M., Daoust, J., Pelletier, M., Biertho, L., Bouvet-Bouchard, L., Fulton, S., Tchernof, A., Dagher, A., Richard, D., Evans, A., Michaud, A., 2022. Impact of weight loss on brain age: Improved brain health following bariatric surgery. NeuroImage 259, 119415. https://doi.org/10.1016/j.neuroimage.2022.119415

Zeighami, Y., Evans, A.C., 2021. Association vs. Prediction: The Impact of Cortical Surface Smoothing and Parcellation on Brain Age. Front. Big Data 4, 15.